Electronic Transport in Y-Junction Carbon Nanotubes

C. Papadopoulos,[1] A. Rakitin,[1] J. Li,[1] A. S. Vedeneev,[1,2] and J. M. Xu[1,3]

[1]*Department of Electrical & Computer Engineering, University of Toronto, 10 King's College Road, Toronto, Ontario, Canada M5S 3G4*
[2]*Russian Academy of Sciences, Institute of Radioengineering and Electronics, Fryazino, Moscow district 141120, Russia*
[3]*Division of Engineering, Brown University, Providence, Rhode Island 02912*
(Received 22 February 2000)

Electronic transport measurements were performed on Y-junction carbon nanotubes. These novel junctions contain a large diameter tube branched into smaller ones. Independent measurements using good quality contacts on both individual Y junctions and many in parallel show intrinsic nonlinear transport and reproducible rectifying behavior at room temperature. The results were modeled using classic interface physics for a junction with an abrupt change in band gap due to the change in tube diameter. These Y-junction tubes represent new heterojunctions for nanoelectronics.

PACS numbers: 73.61.Tm, 61.46.+w, 73.40.Ei, 85.30.Kk

As the trend towards smaller electronic devices continues, the search for alternatives to silicon technology has heightened [1]. The great success of the microelectronics industry has been based on the miniaturization of a few basic device elements which are based on different types of junctions; whether it be the *p-n* junction in diodes, the heterojunction in transistors, or the metal-oxide-semiconductor junction used in most silicon circuits [2]. These junctions possess nonlinear current-voltage (*I-V*) characteristics which allow signal processing to be performed. Achieving similar functionality at the nanometer scale is a primary goal for nanoelectronics.

Carbon nanotubes (CNTs) are a class of nanostructures being explored for molecular-scale devices [3]. These nanostructures can be synthesized by arc discharge [4], laser vaporization [5], and chemical vapor deposition (CVD) [6]. Single-electron devices [7,8] and field-effect transistors [9,10] have been shown by placing straight CNTs across patterned gate electrodes. A different approach to forming nanotube devices involves connecting different tubes to form nanoscale junctions which possess intrinsic device functionality [11–13]. However, for this approach to be successful, the controlled production of such synthetic CNT junctions will be required [13]. A template-based CVD technique has recently been developed that allows the reproducible and high-yield fabrication of Y-junction CNTs [14]. In this Letter, we report conductance measurements on Y-junction CNTs which show intrinsic nonlinear and asymmetric *I-V* behavior at room temperature. These Y-junction CNTs, in which different diameter tubes join in a "Y" structure, represent a new type of nanoscale junction.

The Y-junction CNTs were produced by CVD growth in branched nanochannel alumina templates [14]. This method produces multiwalled CNTs in aligned arrays with adjustable "stem" and "branch" tube diameters (Fig. 1). We performed electronic transport measurements on both arrays and individual Y junctions. The Y junctions were

typically 6 to 10 μm in total length, and tubes with stem/branch diameter ratios of ~50/35 and 60/40 nm were used. Array densities were 10^{10} cm^{-2}.
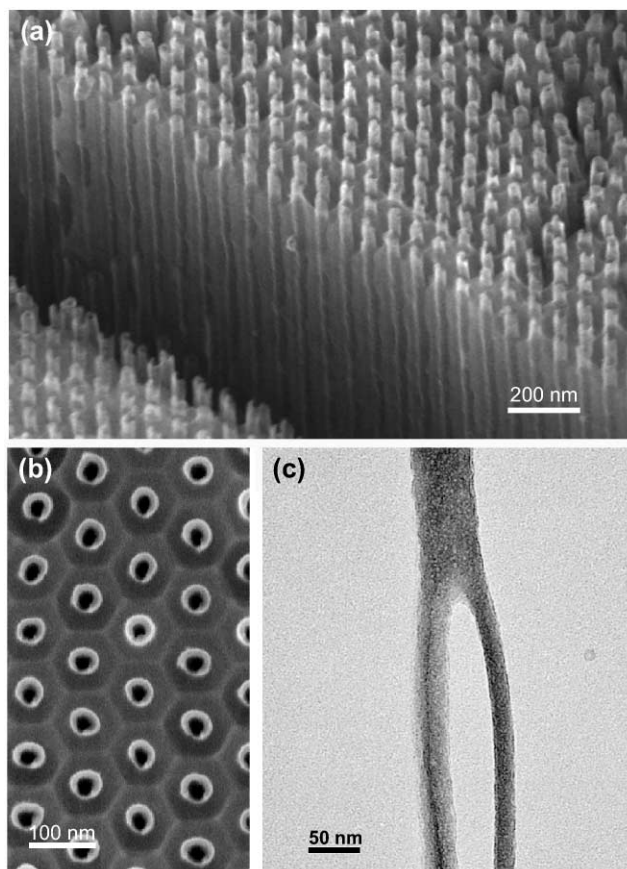
FIG. 1. Y-junction carbon nanotubes grown by CVD in nanochannel alumina templates. (a) Scanning electron micrograph of Y-junction CNT array as viewed from the large diameter stem side. (b) Scanning electron micrograph showing a top view of the array. (c) Transmission electron micrograph of a Y-junction tube removed from the template.
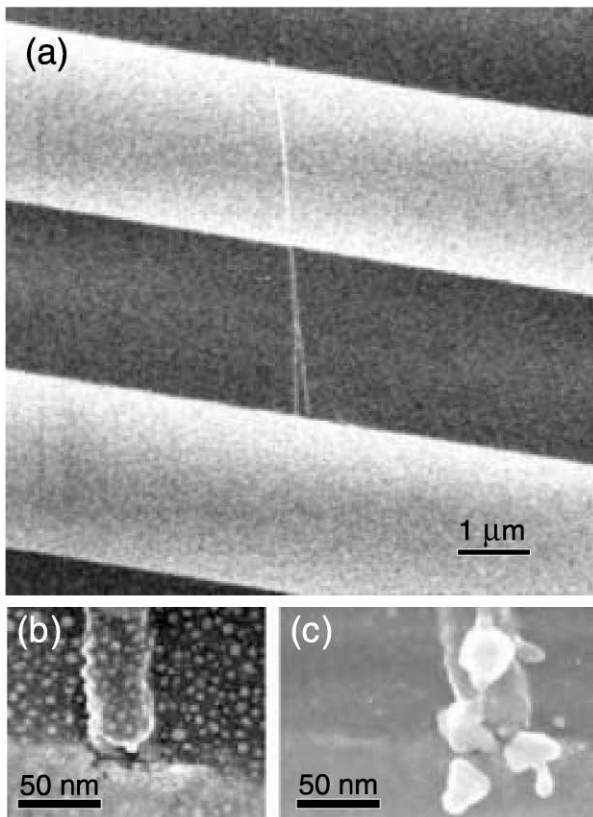
FIG. 2. Y-junction contacts. (a) Scanning electron micrograph of a 6 μm long Y-junction tube across gold electrodes. (b) Tube end showing islandlike gold film. (c) Tube end after application of 10 V for $\sim$90 min and limiting current to $\sim$1 μA. After reaching the saturation current, the bias was gradually decreased and held in a series of steps until the current was observed to be constant at each step. The high local electric field at the tube tip induces the migration of gold particles, forming a low-resistance contact to the electrode.

For electronic transport measurements on individual Y junctions, they were chemically removed from their growth template [15] and dispersed onto patterned electrodes [Fig. 2(a)]. To make low resistance contacts to the Y junction, we first sputtered an islandlike film of gold (or silver) onto the sample [Fig. 2(b)]. Next, a large bias (typically 10 to 20 V, while limiting current) was applied between the two electrodes containing the Y junction. Initially, no current flow was observed; however, over a period of 1–3 hours, the current increased and eventually saturated to a fixed value. Subsequent examination of the tube ends revealed a migration of gold particles [Fig. 2(c)], presumably induced by the high electric field at the tube tips. Similar methods have been used to form Ohmic contacts to C_{60} films via the field enhanced diffusion of gold [16]. We found this method produced reliable and reproducible contacts to individual Y-junction nanotubes. A typical *I-V* plot for an individual Y-junction tube is shown in Fig. 3. The *I-V* data displays distinct asymmetric and rectifying behavior with current flowing more easily under negative bias.
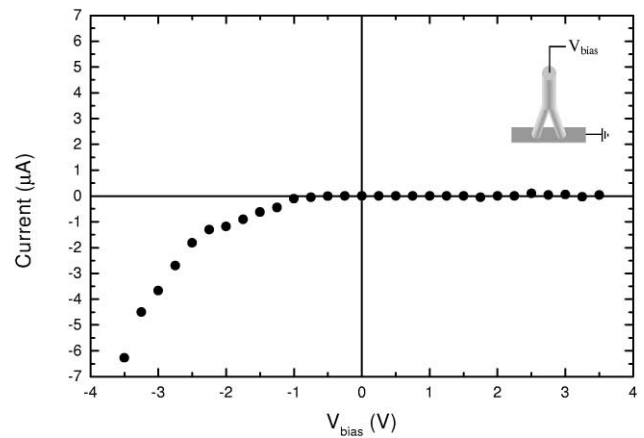
FIG. 3. *I-V* curve for an individual Y-junction nanotube with 50/35 nm stem/branch diameter ratio. The current under negative bias increases rapidly while under positive bias almost zero current was observed. The inset shows the bias configuration used.

For independent confirmation and a statistical distribution of the Y-junction electronic transport, a unique opportunity is afforded by measuring them in their arrays [Fig. 4(a)]. The high density of tubes allowed us to contact and measure the *I-V* characteristics of $\sim$10^2 to 10^8 (depending on contact size) Y junctions in parallel. This allows a large sampling of the Y-junction properties and also permits their uniformity to be judged. In Fig. 4(b), a representative *I-V* curve of $\sim$10^2 junctions connected in parallel is shown. As expected the measured currents are larger, also smoother, due to averaging over many Y junctions. However, the asymmetry and nonlinearity observed for the individual tubes is still evident in the array measurements. This provides verification that the observed behavior is intrinsic to the Y-junction structure of the tubes and shows the tubes are very uniform. To assess the effect of contacts, we performed similar measurements on arrays of straight CVD-grown CNTs. As shown in the inset of Fig. 4(b), the straight tubes display a very linear *I-V* characteristic that is symmetric, providing more evidence that the observed rectifying behavior is an inherent property of the Y-junction tubes.

The room temperature Y-junction CNT *I-V* behavior is remarkable, as only the tube diameter changes across the Y-junction: Measurements on straight multiwalled nanotubes have shown them to be semiconducting with a band gap that is inversely proportional to the diameter [17,18]. In addition, semiconducting CNTs have been shown to be *p* doped [9,10]. Since the Y-junctions were grown by a CVD method known to produce semiconducting tubes [19], we model the Y-junction CNT as a *p-p* isotype semiconductor heterojunction using standard heterostructure physics [20]: The large band gap side of the junction corresponds to the narrow diameter branch tubes and the small band gap side corresponds to the large diameter stem [Fig. 5(a)]. At equilibrium, the Fermi level
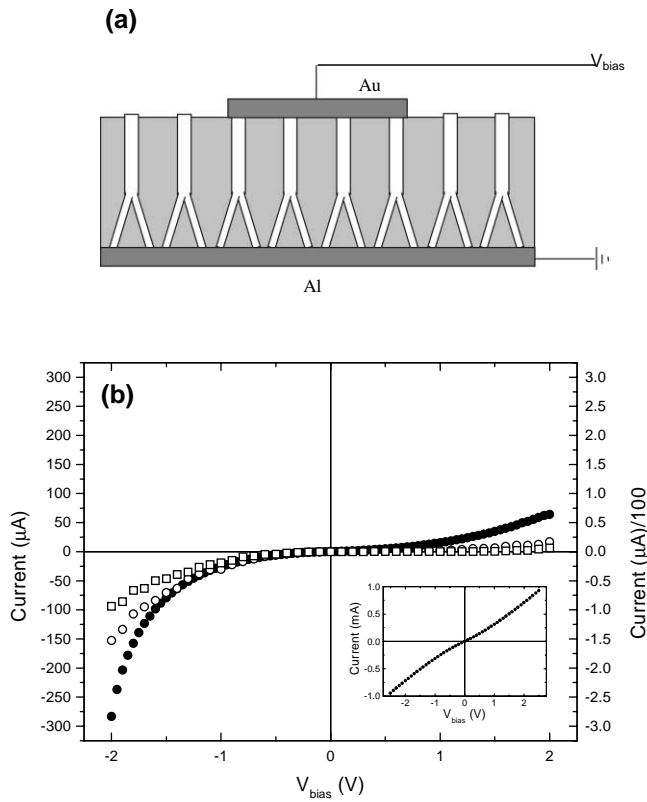
FIG. 4.   Y-junction CNT array *I-V* measurements for tubes with 60/40 nm stem/branch diameter ratios. (a) Contacts to the Y-junction array were made by sputtering gold electrodes using a shadow mask on the stem side of the array and using the native aluminum electrode at the base of the array. (b) *I-V* curves for Y-junction arrays displaying asymmetry and rectification similar to individual tubes. The data (●) corresponds to about 100 junctions measured in parallel and results for different samples scaled down by factors of 10 (○) and 3 (□), corresponding to the approximate number of tubes measured (1000 and 300, respectively), are also shown. The inset shows results obtained for straight tube arrays.

is constant across the junction, and this is accomplished by transfer of holes from the large band gap side to the small band gap side which causes the bands to bend. Under forward bias [Fig. 5(b)] the Fermi level shifts, lowering the barrier to holes and allowing current to increase rapidly. This physical picture agrees qualitatively with our results [Figs. 3 and 4(b)], with large current flowing under forward bias, (negative applied voltage), "pulling" positively charged holes across the junction. Under reverse bias (positive voltage) a small current is observed, and most junctions lost blocking between 3 to 4 V.

For a quantitative picture, we follow the standard Anderson approach [21]: Assuming Boltzmann statistics and using global charge neutrality, Poisson's equation for the stem side of the junction is ($k_B = 1$)

$$\varepsilon_1 \frac{\partial^2 \widetilde{V}_1}{\partial x^2} = 4\pi q N_1 (1 - \exp[-q\widetilde{V}_1/T]). \qquad (1)$$
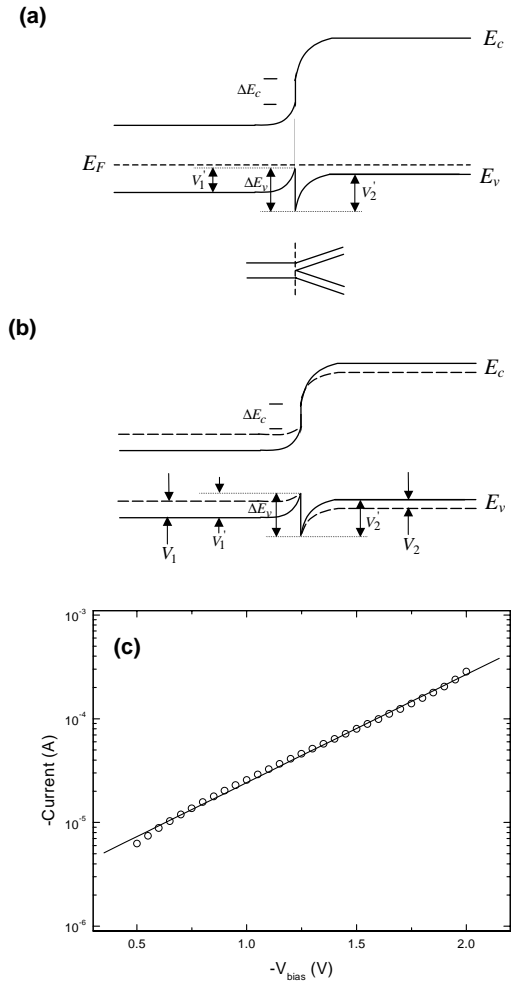
FIG. 5.   Proposed *p-p* isotype heterojunction band-edge diagram for Y-junction CNT. (a) Junction in equilibrium; ΔE_c and ΔE_v represent the conduction and valence band energy offsets, and E_F is the Fermi energy. The difference in band gaps is given by $\Delta E_g = \Delta E_c + \Delta E_v$. The wide band gap side corresponds to the small diameter branches and the narrow band gap side to the larger diameter stem, as indicated. (b) Junction under forward bias (dashed lines); the Fermi energy splits by $eV_{bias} = e(V_1 + V_2)$, reducing the barrier to hole transport. (c) Logarithmic plot of I vs V_{bias} for Y-junction CNT array data shown in Fig. 4(b) (●) under large forward bias and fit to data giving $\eta \sim 17$ [21].

The branch side is almost depleted near the junction, allowing one to simplify its Poisson's equation to [20]

$$\varepsilon_2 \frac{\partial^2 \widetilde{V}_2}{\partial x^2} = 4\pi q N_2, \qquad (2)$$

where $\widetilde{V}_{1,2} = V_{1,2} - V'_{1,2}$, $V_{1,2}$ being the part of the applied voltage V in the stem (branch) side, $V'_{1,2}$ is the built-in potential barrier on either side of the junction, $N_{1,2}$ is the concentration of holes in the stem (branch) far from the junction, $\varepsilon_{1,2}$ is the corresponding dielectric constant, q is the electronic charge, and T is the thermodynamic temperature. Equation (1) can be solved yielding

$$\frac{\partial \tilde{V}_1}{\partial x} = \left(\frac{8\pi q N_1}{\varepsilon_1} \left\{ \tilde{V}_1 + \frac{T}{q} \left[\exp\left(-\frac{q\tilde{V}_1}{T}\right) - 1 \right] \right\} \right)^{1/2}. \tag{3}$$

Using the continuity condition, under relatively large forward bias ($V_1 \gg V_1' \gg T/q$, $V_2 \gg V_2'$), Eqs. (2) and (3) result in the simple relation ($V = V_1 + V_2$)

$$\varepsilon_2 N_2 V_2 = \varepsilon_1 N_1 (V - V_2). \tag{4}$$

Furthermore, it follows from this model [21] that the current under large forward bias varies as

$$I \propto \exp[qV_2/T]. \tag{5}$$

Combining Eqs. (4) and (5) yields

$$I \propto \exp(qV/\eta T), \tag{6}$$

where $\eta = 1 + \varepsilon_2 N_2 / \varepsilon_1 N_1$ is a parameter which depends on the material properties on either side of the interface.

In Fig. 5(c) we show a typical fit of our experimental data. The data agrees well with the Anderson model. From similar fits to the conductance data of individual and array Y-junction samples, we found that η lies in the range 16 to 23. To extract more information about the Y-junction properties, we consider two limiting cases for the dielectric constant ε, i.e., low and high hole concentrations [22]: For low hole concentrations, the fits give N_2/N_1 between 15 and 22, while for high hole concentrations N_2/N_1 lies between 4 and 5. To assess which case may be prevalent in Y-junction CNTs, we consider theoretical calculations based on a "self-doping" model [18] which predict ($D \gg a$, a being the lattice constant)

$$\frac{N_2}{N_1} \sim \left[\frac{D_1}{D_2} \right]^4 \tag{7}$$

for degenerately doped nanotubes [23]. For our experiments, this gives N_2/N_1 between 4 and 5, which implies that hole carriers may provide the main contribution to the dielectric constant [24]. However, both cases are consistent with the Y-junction structure in which the larger diameter stem tube (D_1) resembles graphite and is more lightly doped relative to the smaller diameter branches.

The Y-junction CNT electrical transport characteristics presented here show robust and reproducible rectification at room temperatures, from individual tubes to many connected in parallel. In addition, our results naturally lead the way to a three-terminal nanoscale transistor by applying different voltages to each of the Y-junction arms. More detailed models of transport in the Y-junction tube should assess the effect of defects and disorder [25] and possible coherent effects [26]. Nevertheless, it is intriguing that semiconductor heterojunctions, ubiquitous in conventional microelectronics, can be realized using nanometer scale Y-junction CNTs and that their behavior can be explained simply by considering the change in band gap across the junction caused by joining together different diameter nanotubes.

[1] *Future Trends in Microelectronics: The Road Ahead,* edited by S. Luryi, J. M. Xu, and A. Zaslavsky (Wiley, New York, 1999).
[2] S. M. Sze, *Physics of Semiconductor Devices* (Wiley, New York, 1981).
[3] C. Dekker, Phys. Today **52**, No. 5, 22 (1999).
[4] S. Iijima, Nature (London) **354**, 56 (1991).
[5] A. Thess *et al.,* Science **273**, 483 (1996).
[6] W. Z. Li *et al.,* Science **274**, 1701 (1996).
[7] S. J. Tans *et al.,* Nature (London) **386**, 474 (1997).
[8] M. Bockrath *et al.,* Science **275**, 1922 (1997).
[9] S. J. Tans, A. R. M. Verschueren, and C. Dekker, Nature (London) **393**, 49 (1998).
[10] R. Martel, T. Schmidt, H. R. Shea, T. Hertel, and Ph. Avouris, Appl. Phys. Lett. **73**, 2447 (1998).
[11] L. Chico, V. H. Crespi, L. X. Benedict, S. G. Louie, and M. L. Cohen, Phys. Rev. Lett. **76**, 971 (1996).
[12] M. Menon and D. Srivastava, Phys. Rev. Lett. **79**, 4453 (1997).
[13] Z. Yao, H. W. Ch. Postma, L. Balents, and C. Dekker, Nature (London) **402**, 273 (1999).
[14] J. Li, C. Papadopoulos, and J. M. Xu, Nature (London) **402**, 253 (1999).
[15] J. Li, C. Papadopoulos, J. M. Xu, and M. Moskovits, Appl. Phys. Lett. **75**, 367 (1999).
[16] L. Firlej, N. Kirova, and A. Zahab, Phys. Rev. B **59**, 16 028 (1999).
[17] C. H. Olk and J. P. Heremans, J. Mater. Res. **9**, 259 (1994).
[18] A. Rakitin, C. Papadopoulos, and J. M. Xu, Phys. Rev. B **61**, 5793 (2000).
[19] We performed field effect experiments on CVD-grown CNTs and found the sign of the gate voltage used to modulate the conductance implies semiconducting behavior with hole conductivity at room temperature.
[20] A. G. Milnes and D. L. Feucht, *Heterojunctions and Metal-Semiconductor Junctions* (Academic Press, New York, 1972).
[21] *Electronic Structure of Semiconductor Heterojunctions,* edited by G. Margaritondo (Kluwer, Boston, 1988).
[22] For small hole concentrations, the dielectric constant is determined by a polarization term (ε being N independent), while for large concentrations a Drude-like contribution ($\varepsilon \sim N$) dominates. The former case gives $\eta = 1 + N_2/N_1$, while the latter yields $\eta = 1 + (N_2/N_1)^2$.
[23] A. Rakitin, C. Papadopoulos, D. N. Davydov, and J. M. Xu (to be published).
[24] References [9] and [10] measured relatively large hole carrier concentrations in straight CNTs of $\sim 1 \times 10^7$ cm^{-1} which provides further support for this interpretation.
[25] B. A. Aronzon, E. Z. Meilikhov, D. A. Bakaushin, A. S. Vedeneev, and V. V. Rylkov, JETP Lett. **66**, 668 (1997).
[26] A. S. Vedeneev *et al.,* in Proceedings of the 1999 IEEE International Electron Devices Meeting, Washington, DC, 1999.